Supplementary Material

Tuned Schottky barrier of CoP co-catalyst via the bridge of ohmic contact form Mo metal for enhanced photocatalytic hydrogen evolution

Ying-jie Sun‡, Xue-ting Liu‡, Xin-jie Zhao, Xiao-jing Wang*, Jun Zhao, Yu-pei Li, Hui-ying Mu, Fa-tang Li*

Hebei Key Laboratory of Photoelectric Control on Surface and Interface, College of Science, Hebei University of Science and Technology, Shijiazhuang, 050018, China

‡ These authors contributed equally to this work

** Corresponding authors. E-mail: propyl@163.com (Xiao-jing Wang) and lifatang@126.com (Fa-tang Li)*

S1. Characterization

The crystal structures of the samples were characterized using an X-ray powder diffractometer (Rigaku D/Max 2500). The microstructure and morphology of the samples were recorded by transmission electron microscopy (TEM, JEOL JEM-2100) and scanning electron microscopy (SEM, Hitachi S-4800). High resolution transmission electron microscopy (HRTEM, FEI Talos F200S) was used to test the composition and crystal structure of the samples. The composition, chemical states and valence bands of the elements were tested using X-ray photoelectron spectroscopy (XPS, PHI 1600 ESCA). Photoluminescence (PL) measurements were performed on a fluorescence spectrophotometer (Hitachi F-4600) with an excitation wavelength of 340 nm. The light absorption properties of the samples were tested using an ultraviolet visible (UV-Vis) diffuse reflection spectrophotometer (Thermo Scientific Evolution 220). The Ultraviolet Photoelectron Spectroscopy (UPS) of samples was recorded by (Thermo ESCALAB 250XI). The molecular structure information was conducted on a Raman spectrometer (KL325) with 325 nm excitation wavelength. The element content of the samples was obtained using an inductively coupled plasma atomic emission spectroscopy instrument (Thermo Scientific iCAP 6300), and 0.1g of the samples were pretreated using 5 mol/L HNO_3 and diluted before measurement.

S2. Electrochemical test

The photoelectrochemical and electrochemical measurements were carried out by Chenhua CHI 660E electrochemical workstation. In electrochemical testing, a standard three electrode system was used. The FTO coated with catalyst serves as the working electrode, Pt sheet acts as the counter electrode and Ag/AgCl (3mol/L KCl) is used as reference electrode in a Na_2SO_4 electrolyte (0.2 mol/L). A 300 W xenon lamp with a 400 nm cutoff plate is used as the light source for the photocurrent test. Mott-Schottky analyses were performed in the similar electrochemical configuration of the photocurrent tests without light irradiation. The working electrode was prepared by the following method: 4 mg of the powder sample was dispersed into a mixture of 480 μL deionized water, 480 μL ethanol and 40 μL 5% Nafion solution, and then the solution was evenly dispersed by ultrasonic. Then the 30μl solution was dropped on a clean FTO

conductive glass slice with an area of 1.0 cm^{-2}, and dried in an oven at 80℃ for further use.

S3. Calculation method

First-principles calculations are performed by using density functional theory (DFT) implemented in Vienna Ab-initio Simulation Package (VASP).[1] Projector augmented-wave (PAW) pseudopotential is used to account ion-electron interactions.[2] The correlation and exchange terms are described using general gradient approximation (GGA) in the scheme of Perdew−Burke−Ernzerh (PBE) functional.[3] For the surface construction, the g-C_3N_4(001), CoP(002) and Mo（110）surface is cleaved. During the calculation of charge density difference, a slab model consisted of a crystal (002) face of CoP and (110) plane of Mo was established to represent the contact surface between anatase CoP and Mo. The vacuum separation larger than 15 Å is employed in order to eliminate interactions between two adjacent unit cell. During all calculations, the kinetic energy cutoff of 500 eV is used, and the convergence criteria for energy and force are 10^{-5} eV and 0.03 eV/Å, respectively.

S4. Photocatalytic activity tests

The photocatalytic HER activity of the samples was determined by side irradiation of a 300w Xenon lamp with a 400nm cut-off filter in a self-made quartz reactor under continuous agitation conditions. Generally, 30 mg of photocatalyst sample is added to 30 ml of triethanolamine (TEOA) (20%) aqueous solution as a sacrificial agent. The reaction temperature is constant at 20 ℃, and Ar is used as the carrier gas. The hydrogen production is analyzed by gas chromatography every hour. (Techcomp GC7900, thermal conductivity detector).

The apparent quantum yield (AQY) was tested in a 250 mL quartz top irradiation reactor. Typically, 100 mg of the catalyst, 80 mL of deionized water and 20 mL of triethanolamine were added to the quartz reactor. Other conditions were the same as the photocatalytic experiment except the cut-off filter of the Xe-lamp was change to a 420 ± 20 nm band-pass filter. The effective irradiation area was 19.6 cm^2, the average light intensity was 5.4 $mW \cdot cm^{-2}$ and the irradiation time is 10800s.The AQY was calculated based on the following formula (1):[25]

$$\mathrm{AQY}(\%) = \frac{\text{Number of reacted electrons}}{\text{Number of incident photons}} \times 100\% = \frac{\text{Number of evolved } H_2 \text{ molecules } \times 2}{\text{Number of incident photons}} \times 100\%$$

(1)

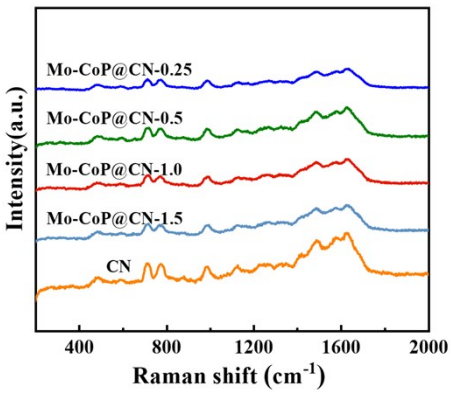

Fig. S1 Raman spectra CN and Mo-CoP@CN composites.

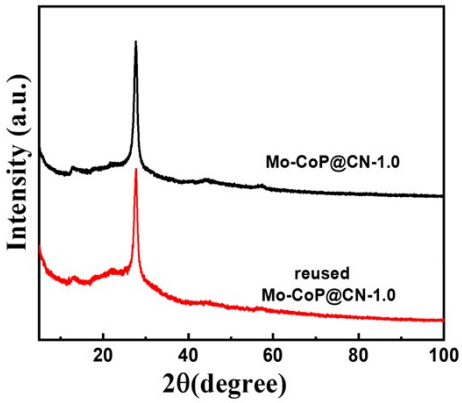

Fig. S2 XRD patterns of Mo-CoP@CN-1.0 before and after recycling.

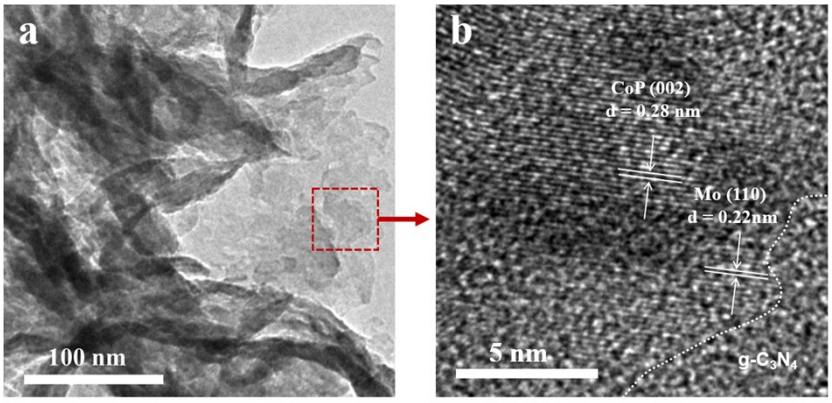

Fig. S3 (a) TEM and (b) HRTEM images of the reused Mo-CoP@CN-1.0

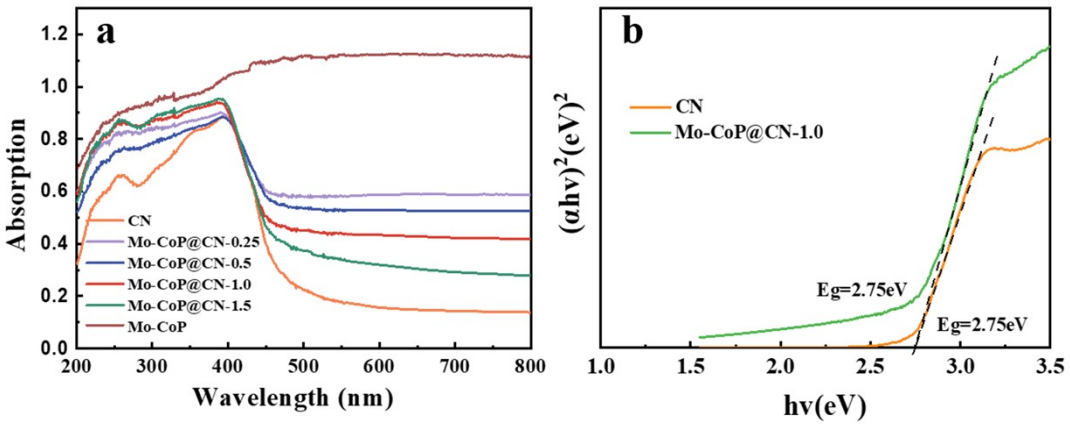

Fig. S4 (a) UV-visible diffuse reflection spectra of different samples (b) Kubelka-Munk function transformation spectra

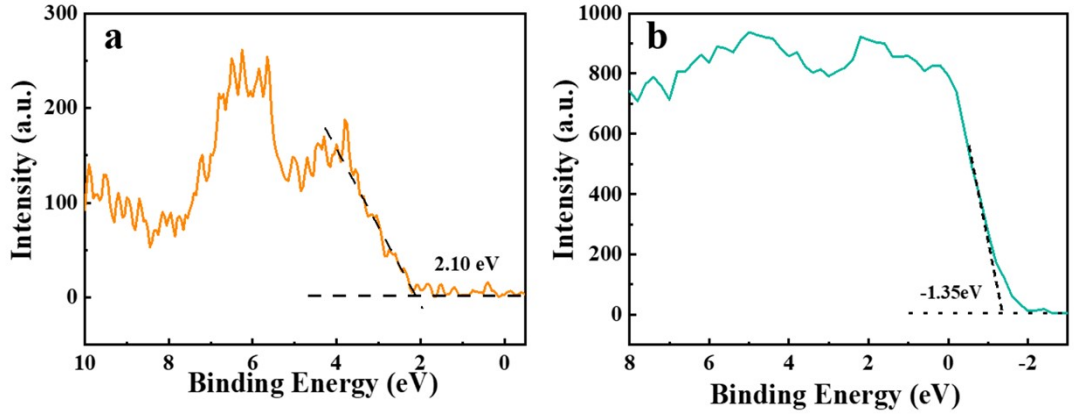

Fig. S5 XPS valence band spectra (a) CN (b) Mo-CoP

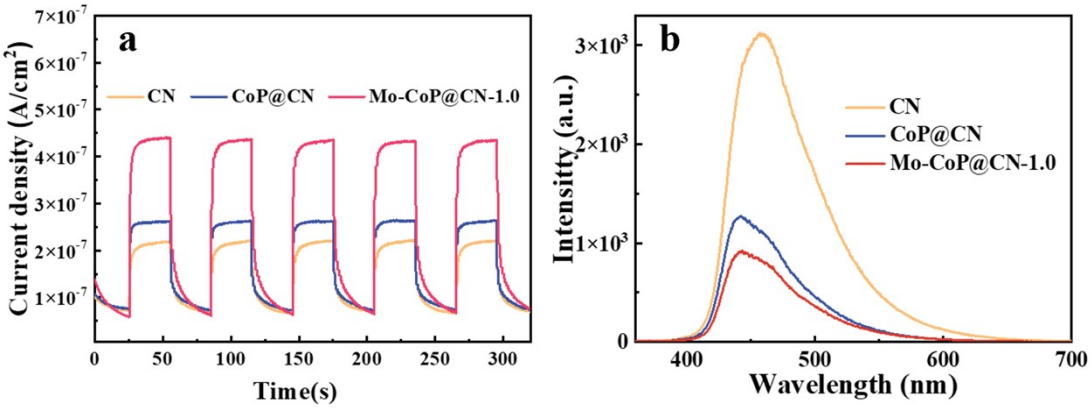

Fig. S6 (a) photocurrent test (b) PL spectrum of CN, CoP@CN, Mo-CoP@CN-1.0.

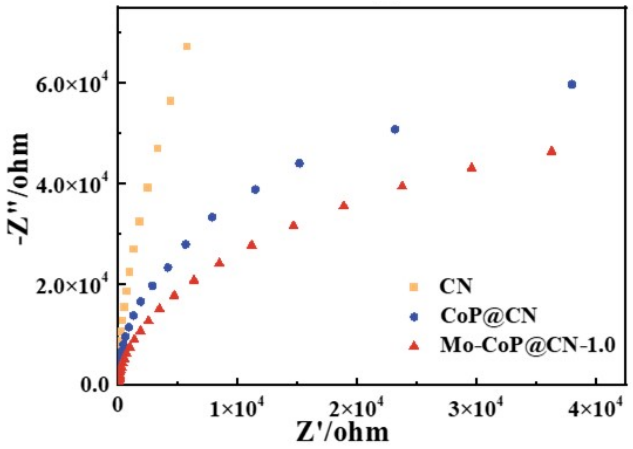

Fig. S7 Electrochemical impedance of CN, CoP@CN, Mo-CoP@CN-1.0.

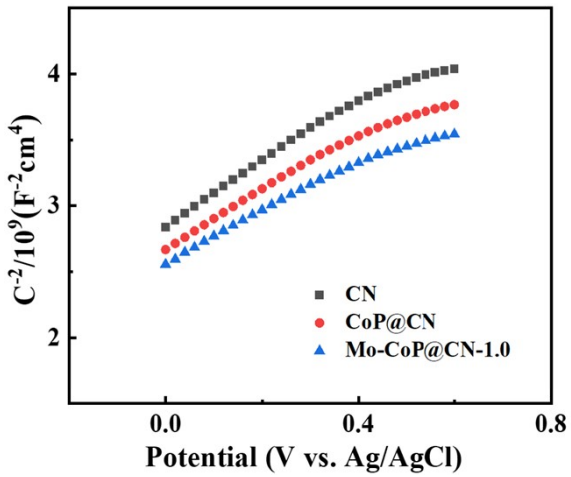

Fig. S8 MS plots of CN, CoP@CN, Mo-CoP@CN-1.0.

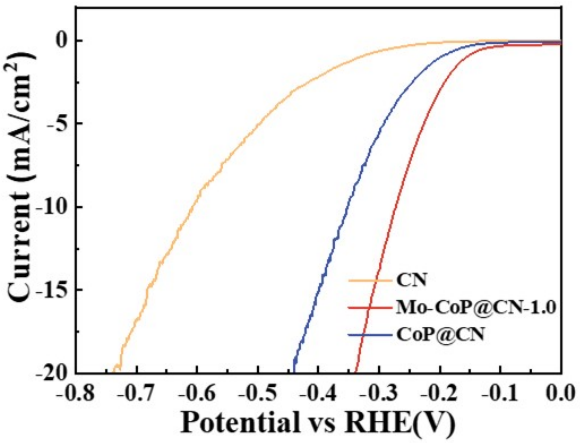

Fig. S9 LSV polarization curve of CN, CoP@CN, Mo-CoP@CN-1.0.

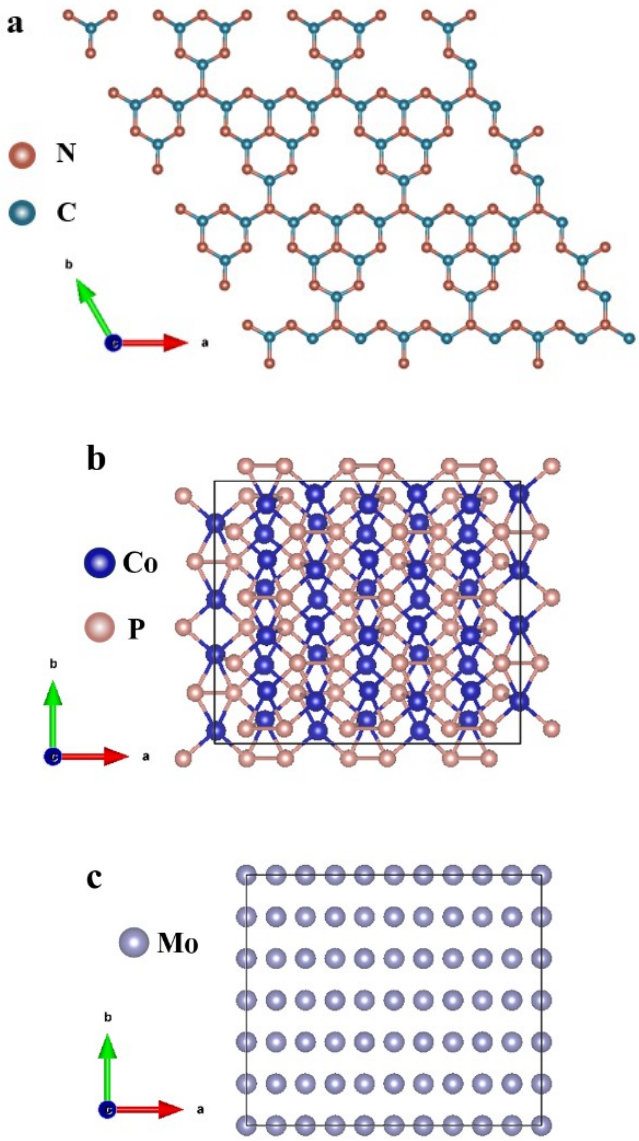

Fig. S10 The crystal structure of (a) g-C_3N_4, (b)CoP, (c) Metal Mo.

Table S1. The Mo, Co and P contents of the as prepared Mo/CoP samples detected by ICP-AES.

Sample	Mo content wt%	Co content wt%	P content wt%	Mo/Co/P molar ratio
Mo/CoP -0.5	17	53	30	1.0/5.0/5.4
Mo/CoP -1	26	46	28	1.0/2.8/3.3
Mo/CoP -1.5	38	40	22	1.0/1.7/1.8

Table S2 The performance comparison of the catalysts from the different references.

Photocatalyst	**Light**	**Sacrificial agent**	**Rate of H_2 Evolution** ($\mu molL \cdot g^{-1} \cdot h^{-1}$)	**AQE at 420 nm**	**Ref.**
Mo-CoP@CN	Xe 300 W, $\lambda > 400$ nm	10%TEOA	1470	5.39%	This work
Ni/g-C_3N_4	Hg 500 W	10% methanol	270	—	4
NiS/g-C_3N_4	LED 3W, $\lambda = 420$ nm	10% TEOA	244	—	5
Ni_3C@Ni/g-C_3N_4	Xe 300W, $\lambda > 420$ nm	15% TEOA	11.28	1.49%	6
NC-Co_3W_3C@g-C_3N_4	Xe 300 W, $\lambda = 400$ nm	15% TEOA	1332	5.12%	7
MoO_2/Ni_2P@g-C_3N_4	Xe 300 W, $\lambda > 400$ nm	10% TEOA	617.2	2.13%	8
UCN-200	Xe 300 W $\lambda > 420$ nm	10% TEOA	1254.75	—	9
$CuInS_2$/g-C_3N_4	Xe 350 W, $\lambda = 365$ nm	10% TEOA	102.4	—	10
$Ni_xCo_{1-x}P$/rGO/CN	Xe 300 W, $\lambda > 420$ nm	PLA	576.7	1.7%	11
OH-HCNMS	Xe 300 W, $\lambda = 420$ nm	10% TEOA	328.9	3.7%	12
Pt SAs/C_3N_4	Xe 300 W	20% TEOA	573.6	—	13
Ag_2S QDs/g-C_3N_4	Xe 300 W, $\lambda > 420$ nm	20% TEOA	471.1	0.82%	14
Co_3O_4/g-C_3N_4	Xe 300 W, $\lambda = 420$ nm	15% TEOA	105.06	0.053%	15
CoS_2/S/g-C_3N_4	Xe 300 W, $\lambda > 420$ nm	10% TEOA	577.5	1.08%	16

References

1. G. Kresse and J. Furthmüller, Efficiency of Ab-initio total energy calculations for metals and semiconductors using a plane-wave basis set. *Comput. Mater. Sci.,* 1996, 6, 15-50.

2. G. Kresse and D. Joubert, From ultrasoft pseudopotentials to the projector

augmented-wave method. *Phys. Rev. B,* 1999, 59, 1758-1775.

3. J. P. Perdew, K. Burke and M. Ernzerhof, Generalized gradient approximation made simple. *Phy. Rev. Lett.,* 1996, 77, 3865-3868.
4. M. Ismael, One-step ultrasonic-assisted synthesis of Ni-doped g-C_3N_4 photocatalyst for enhanced photocatalytic hydrogen evolution. *Inorg. Chem. Commun.,* 2023, 15, 110607.
5. M. Wang, J. Cheng, X. Wang, X. Hong, J. Fan and H. Yu, Sulfur-mediated photodeposition synthesis of NiS cocatalyst for boosting H_2-evolution performance of g-C_3N_4 photocatalyst. *Chin. J. Catal.,* 2021, 42(1): 37-45.
6. R. Shen, K. He, Zhang A, N. Li, Y. H. Ng, P. Zhang, J. Hu and X. Li, In-situ construction of metallic Ni_3C@Ni Core-Shell cocatalysts over g-C_3N_4 nanosheets for shell-thickness-dependented photocatalytic H_2 production. *Appl. Catal. B: Environ.*, 2021, 291: 120104.
7. X. Zhou, J. Luo, B. Jin, Z. Wu, S. Yang, S. Zhang, Y. Tian, Y. Fang, Y. Hou and X. Zhou, Sustainable synthesis of low-cost nitrogen-doped-carbon coated Co_3W_3C@g-C_3N_4 composite photocatalyst for efficient hydrogen evolution. *Chem. Eng. J.,* 2021, 426 (2): 131208.
8. X.T. Liu, B. H. Li, X. J. Wang, Y. L. Li, J. Zhao, Y. P. Li, and F. T. Li, Enhanced schottky effect in the Ni_2P cocatalyst via work function up-shift induced by MoO_2 for boosting photocatalytic hydrogen evolution. *ACS Sustainable Chem. Eng.* 2022, 10, 10627−10640
9. L. Chen, X. Liang, H. Wang, Q. Xiao and X. Qiu, Ultra-thin carbon nitride nanosheets for efficient photocatalytic hydrogen evolution. *Chem. Eng. J.,* 2022, 442, 136115.
10. J. Zhang, Y. Zhao, K. Qi and S.Y. Liu, $CuInS_2$ quantum-dot-modified g-C_3N_4 S-scheme heterojunction photocatalyst for hydrogen production and tetracycline degradation. *J. Mater. Sci. Technol.,* 2024, 172,145-155.
11. J. Yan, D. Sun and J. Huang, Synergistic poly (lactic acid) photoreforming and H_2 generation over ternary $Ni_xCo_{1-x}P$/reduced graphene oxide/g-C_3N_4 composite. *Chemosphere,* 2022, 286: 131905.

12. S. Wang, X. Zhao, X. Zhao, J. Zhang, Z. Ao, P. Dong, F. He, H. Wu, X. Xu, L. Shi, C. Zhao, S. Wang and H. Sun, Surface engineering of hollow carbon nitride microspheres for efficient photoredox catalysis. *Chem. Eng. J.,* 2020, 381, 122593.

13. Y. Hu, Y. Qu, Y. Zhou, Z. Wang, H. Wang, B. Yang, Z. Yu, Y. Wu, Single Pt atom-anchored C_3N_4: A bridging Pt-N bond boosted electron transfer for highly efficient photocatalytic H_2 generation. *Chem. Eng. J.,* 2021, 412, 128749.
14. Z. You, X. Yue, D. Zhang, J. Fan and Q. Xiang, Construction 0D/2D heterojunction by highly dispersed Ag_2S quantum dots (QDs) loaded on the g-C_3N_4 nanosheets for photocatalytic hydrogen evolution. *J. Colloid. Interf. Sci.,* 2022, 607, 662-675.
15. Z. Xu, J. Zhong, J. Chen, M. Li, L. Zeng and H. Yang, Construction of S-scheme Co_3O_4/g-C_3N_4 heterojunctions with boosted photocatalytic H_2 production performance. *Surf. Interf.,* 2023, 38, 102838.
16. Y. Z. Zhang, J. W. Shi, Z. X. Huang, X. J. Guan, S. C. Zong, C. Cheng, B. T. Zheng and L. J. Guo, Synchronous construction of CoS_2 in-situ loading and S doping for g-C_3N_4: Enhanced photocatalytic H_2-evolution activity and mechanism insight. *Chem. Eng. J.,* 2020, 401, 26135.